New reactivity of 6,6-bis-donor-substituted pentafulvenes: one-step synthesis of highly substituted [3]cumulene and dihydropentalene

Nicolas Kerisit, Aaron D. Finke, Nils Trapp, Yann R. Leroux, Jean-Claude Guillemin, Yann Trolez, François Diederich

New reactivity of 6,6-bis-donor-substituted pentafulvenes: one-step synthesis of highly substituted [3]cumulene and dihydropentalene

Nicolas Kerisit,[1] Aaron D. Finke,[2] Nils Trapp,[2] Yann R. Leroux,[3] Jean-Claude Guillemin,[1] Yann Trolez,[1] François Diederich[2,*]

[1] Ecole Nationale Supérieure de Chimie de Rennes, CNRS, UMR 6226, 11 allée de Beaulieu, CS 50837, 35708 Rennes Cedex 7, France

[2] Laboratorium für Organische Chemie, ETH Zurich, Vladimir-Prelog-Weg 3, 8093 Zurich, Switzerland. Email: diederich@org.chem.ethz.ch

[3] Institut des Sciences Chimiques de Rennes, CNRS, Université de Rennes 1, UMR 6226, Campus de Beaulieu, 35042 Rennes Cedex, France

Abstract

We report the preparation of a 6,6-bis[(4-*N,N*-dimethylanilino)ethynyl]pentafulvene from a 6,6-dibromopentafulvene and 4-ethynyl-*N,N*-dimethylaniline under Sonogashira cross-coupling conditions. A push-pull [3]cumulene was formed unexpectedly during this reaction in moderate yield. The 6,6-bis[(4-*N,N*-dimethylanilino)ethynyl]pentafulvene was reacted with tetracyanoethylene, and an unprecedented 1,2-dihydropentalene was obtained in high yield as the exclusive product. The structures of the new compounds are supported by X-ray analysis, and a reasonable mechanism for their formation is proposed. We also report their interesting opto-electronic properties, as studied by UV/Vis spectroscopy and cyclic voltammetry (CV).

Keywords: pentafulvenes, [2+2] cycloaddition, electrocyclization, [3]cumulene, dihydropentalene

1. Introduction

The [2+2] cycloaddition-retroelectrocyclization (CA–RE) between electron-rich alkynes and electron-poor olefins has met increasing interest in the scientific community. This reaction, which efficiently generates 1,1,4,4-tetracyanobutadienes (TCBD) when using tetracyanoethylene (TCNE), is the source of several materials with outstanding opto-electronic properties (Scheme 1).[1] However, in some cases, the reaction between TCNE and electron-rich alkynes does not lead to the expected TCBD but to other products that may be attributed to the reactivity of TCBDs themselves or to other chemical pathways, thereby expanding the chemical diversity of push-pull chromophores and opening new horizons in opto-electronics.[2]

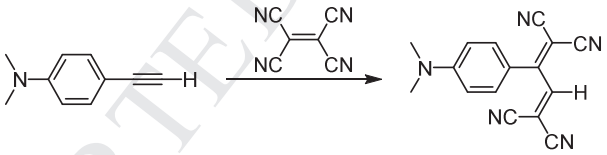

Scheme 1. CA–RE reaction of 4-ethynyl-*N*,*N*-dimethylaniline with TCNE.

We have recently investigated 6,6-dicyanopentafulvenes (DCFs) for their unique electron-accepting properties.[3] We discovered a diverse array of new reactivities of DCFs, many of which led to the formation of chromophores with interesting opto-electronic properties.[4] Moreover, DCFs also showed novel reactivity with *p*-anilino-substituted alkynes in the CA–RE reaction, displaying a strong dependence of ancillary substitution on regioselectivity,[5] and, in one case, led to the formation of even more complex products.[6]

The exciting chemistry of acceptor-substituted pentafulvenes[7] led us to explore the electronic properties and reactivity of pentafulvenes substituted by donors at the exocyclic double bond. We report herein the preparation of a 6,6-bis[(4-*N,N*-dimethylanilino)ethynyl]pentafulvene **1** and an unanticipated [3]cumulene **2** as a side product. We also describe the formation of an unexpected 1,2-dihydropentalene (±)-**3** upon reaction of the aforementioned pentafulvene **1** with TCNE in very good yield.

2. Results and discussion

2.1. Synthesis of pentafulvene 1 and [3]cumulene 2

The synthesis of pentafulvene **1** and [3]cumulene **2** started with the reaction of tetraphenylcyclopentadienone and tetrabromomethane in the presence of triisopropyl phosphite to give 6,6-dibromofulvene **4** in 18% yield (Scheme 2). Recently, Tykwinski *et al.* reported the preparation of **4** with CBr_4/PPh_3 in better yield, but we found that using $P(O\textit{i}Pr)_3$ led to easier purification.[8] Compound **4** was then submitted to a double cross-coupling with 4-ethynyl-*N,N*-dimethylaniline under Sonogashira conditions using $[PdCl_2(PPh_3)_2]$ and CuI as co-catalysts and triethylamine as solvent and base. The expected product **1** was obtained as the major product in 22% yield. However, a second product, sapphire blue in color, was also obtained in 18% yield. Its molecular formula as determined by HR-MS corresponded to an isomer of **1**. The structure was unambiguously elucidated as [3]cumulene **2** by single-crystal X-ray diffraction (Fig. 1). To the best of our knowledge, there are just two reports describing structures with a pentafulvene scaffold where the exocyclic double bond is part of a [3]cumulene.[9]

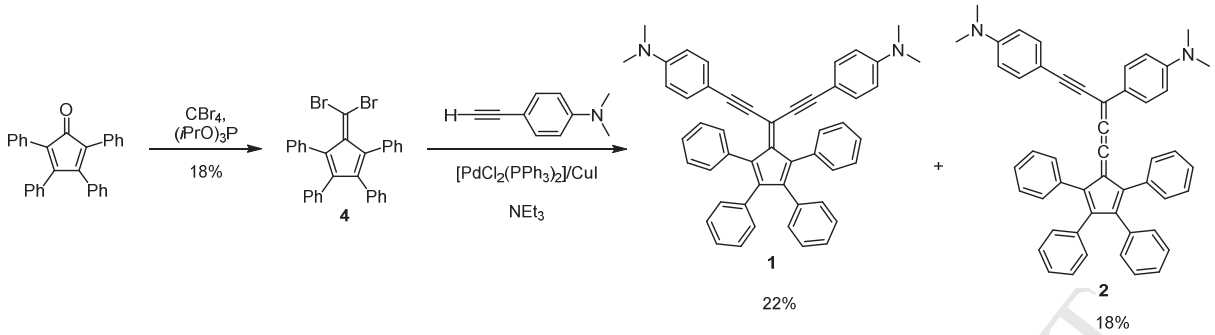

Scheme 2. Synthesis of compound **4** and one-pot synthesis of compounds **1** and **2**.

Both compounds **1** and **2** were characterized by X-ray diffraction (Fig. 1). In the two structures, the dimethylanilino rings are approximately in the same plane as the pentafulvene core, which suggests that there is π-conjugation between the dimethylanilino rings and the cyclopentadiene ring. The four phenyl rings on the cyclopentadiene ring are significantly twisted out of the plane defined by the pentafulvene core, due to steric congestion. The phenyl rings A and D in **1** (torsion angles of 70° and 84°, respectively) are more out o f plane than those in **2** (torsion angles of 44° and 48°, respectively). This can be e xplained by the proximity between the dimethylanilino (DMA) rings F and E and the phenyl rings A and D in **1** as compared to **2**. The quinoid character[10] δr of the donor rings E and F in **1** and **2** was determined from the X-ray bond lengths (see the Supporting Information). The δr values obtained for the anilino rings of **1** are 0.028 Å for F and 0.022 Å for E, which corresponds to a moderate bond length alternation. For **2**, the quinoid character is 0.025 Å for F and 0.038 Å for E. The higher quinoid character of ring E is evidence of stronger π-conjugation between DMA ring E and the cyclopentadiene ring, compared to the ethynylaniline moiety F. This observation is corroborated by the torsion angles of the anilines with respect to the plane of the pentafulvene: 2° for E and 24° for F. The terminal C=C bonds of the butatriene are both 1.36 Å long, and the central C=C

bond is 1.23 Å, which is short and not so different in length from the C≡C triple bond in alkynes. This acetylenic character is less pronounced than in push-pull butatrienes, where the central bond is about 1.21 Å,[11] but slightly more pronounced than in tetraarylbutatrienes, where the central bond is about 1.25 Å.[2e,12]

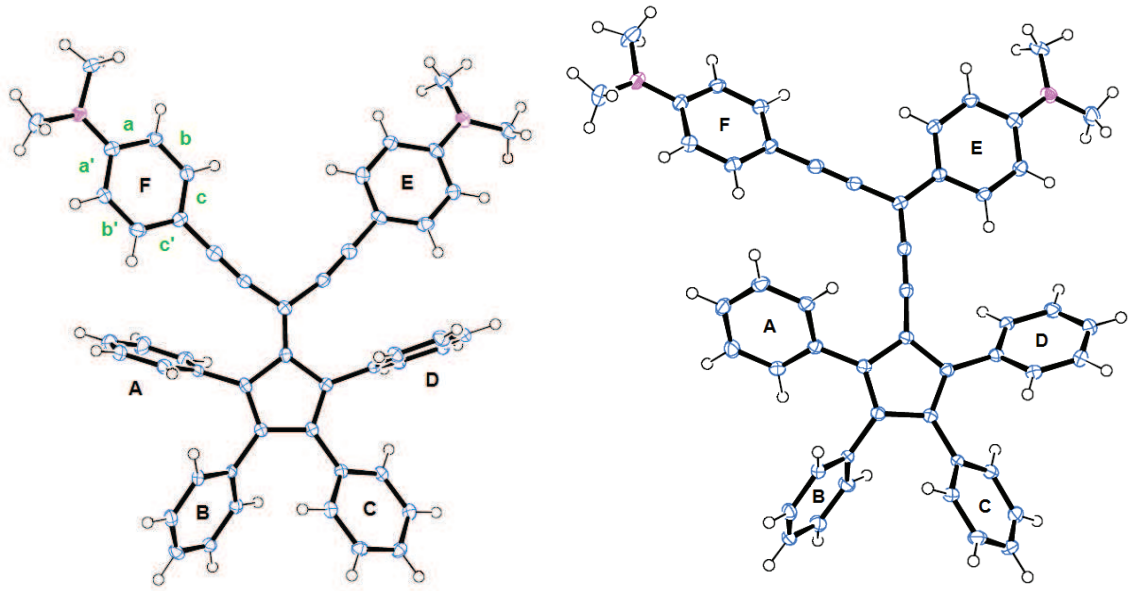

Figure 1. X-ray structures of compounds **1** (left) and **2** (right). Solvent molecules were omitted for clarity. Thermal ellipsoids of non-H atoms at 50% probability. *T* = 100 K.

Even though compound **1** resulted from a classical double Sonogashira coupling, the formation of compound **2** is not so trivial. While **2**, similar to **1**, arises from the coupling of two equivalents of 4-ethynyl-*N,N*-dimethylaniline to **4**, the mechanisms leading to each product clearly diverge somewhere in the course of the reaction. We propose a mechanism of the formation of **2**, shown in Scheme 3. The first step is a simple Sonogashira coupling, following the classical sequence of oxidative addition, transmetallation, and reductive elimination leading to intermediate **4a**. At this point, there are two possibilities: oxidative addition of Pd(0) to the bromide,

leading to a second Sonogashira-type coupling to form **1**, or S_N2' attack by Pd(0), leading to elimination of bromide and formation of [3]cumulene intermediate **2a**.[13] Subsequently, a transmetallation of the copper acetylide occurs, followed by a reductive elimination step to give compound **2**. If the mechanism we propose is correct, the competition between the formation of compound **1** and **2** is related to the difference in the reaction rate between the second oxidative addition of Pd(0) and the S_N2' reaction. Since the yield of the isolated products is approximately the same (22% versus 18%), we may deduce that in this case, the reaction rates of these two steps are comparable. The fact that an unusual S_N2' reaction is competitive with the usual oxidative addition might be linked to the electron-withdrawing character of the fulvene that strongly polarizes the C≡C triple bond, additionally to the presence of the adjacent aniline. To our knowledge, regardless of the mechanism, such a preparation of a [3]cumulene has not been reported to date.

We reacted **2** with TCNE in CH_2Cl_2 at room temperature, but the attempted cycloaddition led to multiple products that could not be characterized.

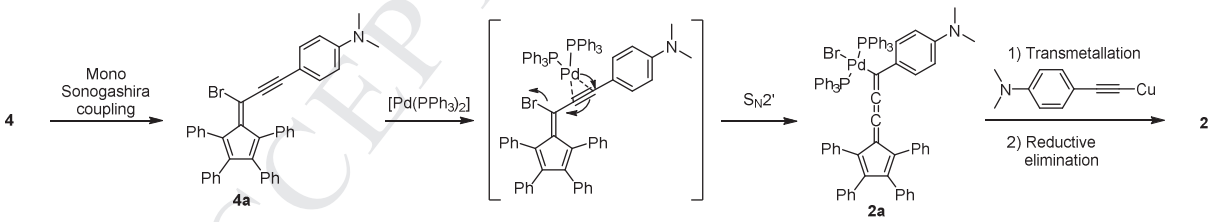

Scheme 3. Proposed mechanism leading to the [3]cumulene **2**.

2.2. Reactivity of pentafulvene 1 with TCNE

The reactivity of pentafulvene **1** with TCNE was then evaluated. One equiv of **1** was mixed with one or two equiv TCNE in dichloromethane. In both cases, the same product (±)-**3** was isolated in the same yield (81%) after column

chromatography. Contrary to what was anticipated, the usual tetracyanobutadiene adduct **5** was not obtained; instead, 1,2-dihydropentalene (±)-**3** was formed and its structure unambiguously determined by single-crystal X-ray diffraction (Fig. 2). We believe that tetracyanobutadiene **5** was formed initially but immediately underwent an electrocyclization involving four C=C double bonds (Scheme 4). Such an electrocyclization of pentafulvenes yielding dihydropentalene has already been described in the literature, even if such reports are very scarce.[14] However, the previous reported electrocyclizations occurred at high temperature (above 100 °C) and not at room temperature.

The second equiv of TCNE did not react with the remaining triple bond probably for steric reasons. The presence of the dicyanovinyl group may also decrease the electronic density on the unreacted triple bond, explaining its lack of reactivity with the second equiv of TCNE. The reaction of **1** with 7,7,8,8-tetracyano-*p*-quinodimethane (TCNQ) was complex and led to multiple products that could not be characterized.

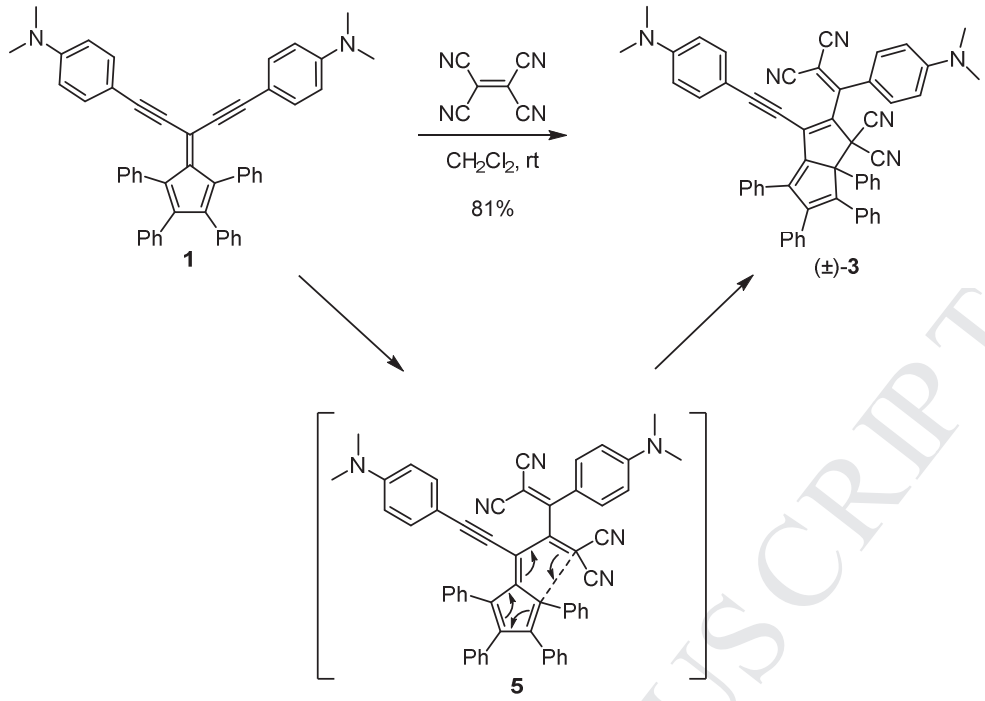

Scheme 4. Formation of dihydropentalene (±)-**3** from pentafulvene **1** and TCNE and its putative reaction pathway.

Dihydropentalene (±)-**3** was characterized by NMR, IR, and UV/Vis spectroscopy, high-resolution mass spectrometry, electrochemistry, and X-ray crystallography (Fig. 2). The solid-state structure of dihydropentalene (±)-**3** shows a torsion angle between the plane of the dicyanovinyl group and the proximate DMA ring E of about 40°, likely due to sterics. The torsion angle between the DMA ring F and the dicyanovinyl moieties is about 47°. The quinoid character for dimethylaniline E, directly connected to the dicyanovinyl moiety is δr = 0.028 Å, and the DMA ring F bearing a C≡C triple bond has a quinoid character of 0.030 Å. These values show that electrons from the more distant aniline are more likely to be delocalized toward the dicyanovinyl moiety, even though the distance is less favorable.

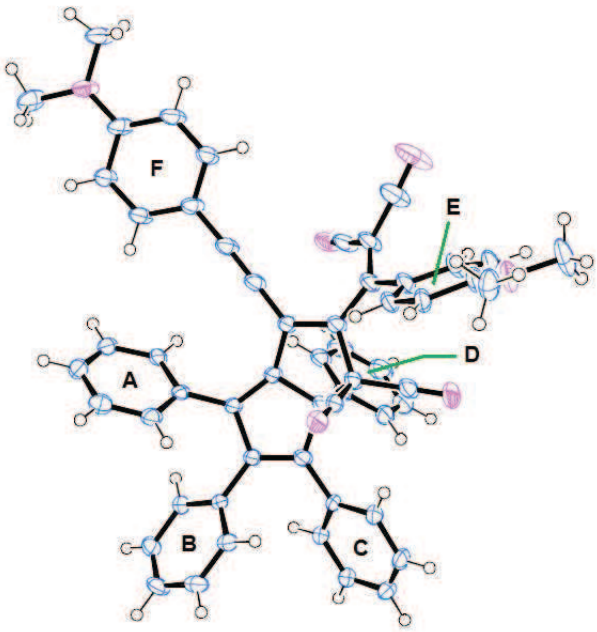

Figure 2. X-ray structure of dihydropentalene (±)-**3**; solvent molecules were omitted for clarity. Thermal ellipsoids of non-H atoms at 50% probability. T = 100 K.

2.3. UV/Vis spectra

The UV/Vis absorption spectra of compounds **1**, **2**, and (±)-**3** were measured at 298 K in dichloromethane (Fig. 3). The strong absorption maximum of compound **1** is located at 491 nm (ε = 5.1 x 10^4 L mol^{-1} cm^{-1}). The optical behavior of compound **2** is striking, with its beautiful sapphire color. [3]Cumulene **2** absorbs light throughout the entire visible range, with large extinction coefficients between 500 and 700 nm. In this region, there are two maxima at λ_{max} = 540 nm (ε = 4.4 x 10^4 L mol^{-1} cm^{-1}) and 631 nm (ε = 4.4 x 10^4 L mol^{-1} cm^{-1}). Such panchromatic systems are very promising for technologies that need to harvest sunlight in the visible region, such as photovoltaic cells. The significant difference in spectra observed between **1** and **2** can be explained by the fact that the conjugated π-system of compound **2** is more extended than that of compound **1**, even though they are constitutional isomers. The absorption spectrum of compound (±)-**3** is more common, with an absorption region

more extended than compound **1** but less intense, with an absorption maximum at 489 nm (ε = 1.8 x 10^4 L mol^{-1} cm^{-1}). Such an absorption spectrum is similar to those of DMA-dicyanovinyl chromophores obtained in CA–RE reactions, both in terms of absorption region and molar extinction coefficients.[15]

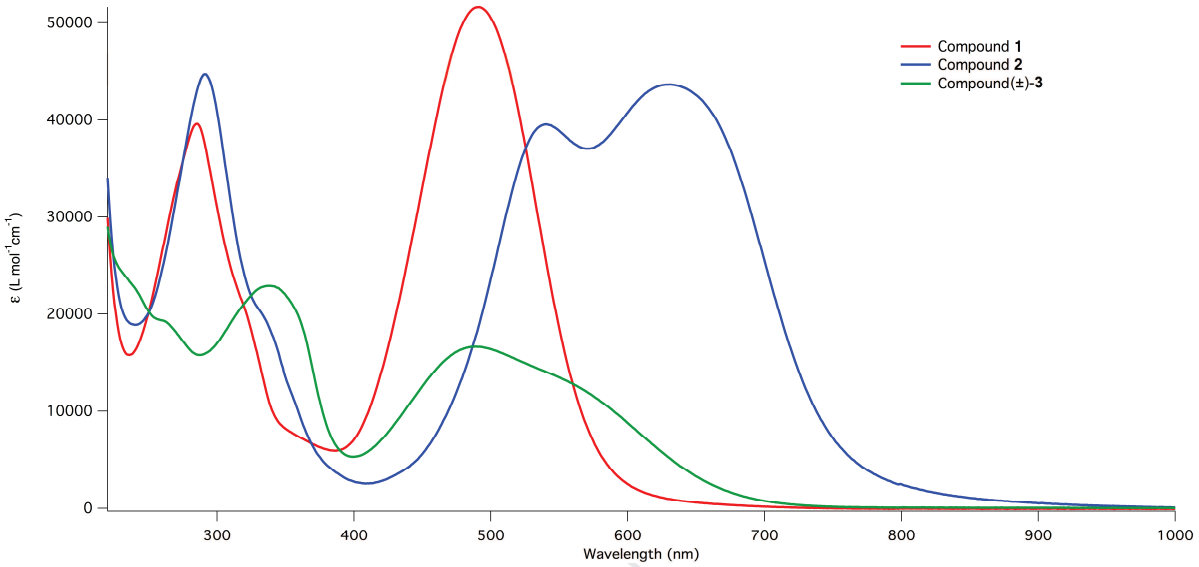

Figure. 3. Absorption spectra of compounds **1** (red line), **2** (blue line), and (±)-**3** (green line) between 220 and 1000 nm, recorded in CH_2Cl_2 at 298 K.

2.4. Electrochemistry

Cyclic voltammograms (CV) were recorded at a scan rate of 0.1 V s^{-1} in CH_2Cl_2 + 0.2 M *n*-Bu_4NPF_6 using ferrocene as external standard, to characterize the redox properties of compounds **1**, **2**, and (±)-**3**. All the potential values are given *versus* the potential of the Fc^+/Fc couple (+0.46 V *vs* SCE). Pentafulvene **1** shows an irreversible oxidation peak at 0.45 V and a quasi-reversible reduction peak at -1.63 V. Interestingly, [3]cumulene **2** exhibits similar behavior but with shifted potentials, with an irreversible oxidation peak at +0.1 V and a quasi-reversible reduction peak at -1.31 V. As expected and in accordance with the optical data, [3]cumulene **2** shows a

smaller electrochemical energy gap of around 1.41 eV, compared to its isomer **1** exhibiting an electrochemical energy gap of 2.08 eV. Dihydropentalene (±)-**3** exhibits an irreversible oxidation at a potential close to that of pentafulvene **1** at +0.56 V and a more facilitated two-electron reduction at -1.08 V, associated with two successive one-electron transfer oxidation steps. Dihydropentalene (±)-**3** shows an electrochemical energy gap around 1.64 eV. Whereas the energy gap difference between pentafulvene **1** and its isomer, [3]cumulene **2**, is affected by shifts of both HOMO and LUMO energies, the decrease in energy gap between pentafulvene **1** and dihydropentalene (±)-**3** is dominated by the change in the LUMO energy, while its HOMO energy remains close to the one of pentafulvene **1**. The calculated optical gap and electrochemical gaps are in good accordance, which may indicate that the lowest-energy absorption is associated with the HOMO-LUMO transition for the three different compounds.

Table 1

Overview of the first reduction and oxidation potentials from cyclic voltammetry (CV) and summary of electrochemical and optical energy gaps.

Compound	E_{ox} (V)[a]	E_{red} (V)[a]	ΔE_{redox} (eV)[d]	λ_{onset} (nm)	ΔE_{opt} (eV)[e]	HOMO[f] (eV)	LUMO[f] (eV)
1	**0.45**[b]	**-1.63**[c]	2.08	620	2.00	-5.3	-3.2
2	**0.10**[b]	**-1.31**[c]	1.41	850	1.46	-4.9	-3.5
(±)-**3**	**0.56**[b]	**-1.08**[c]	1.64	728	1.70	-5.4	-3.7

[a] Electrochemical data obtained at a scan rate of 0.1 V s^{-1} in CH_2Cl_2 + 0.2 M *n*-Bu_4NPF_6 on a glassy carbon working electrode. All potentials are given *versus* the Fc^+/Fc couple used as external standard. Complete set of electrochemical data, including second oxidation and reduction potentials (when detected) can be found in the Supporting Information. [b] Irreversible peak potential. [c] Redox potential for reversible electron transfer. [d] The electrochemical gap, ΔE_{redox}, is defined as the potential difference between the first oxidative onset potential and the first reductive onset potentials. [e] The optical gap, ΔE_{opt}, is defined as the energy corresponding to

the lowest-energy absorption (λ_{onset}). [f] HOMO and LUMO energy levels are determined from electrochemical measurements. See Supporting Information for details.

3. Conclusions

The Pd-catalyzed Sonogashira cross-coupling between 6,6-dibromo-1,2,3,4-tetraphenylpentafulvene with DMA-acetylene afforded not only the expected doubly coupled product **1** but also [3]cumulene **2** in nearly identical, modest yield. The structures were characterized by X-ray diffraction, and a mechanism for the formation of **2** was proposed based on an S_N2' attack of Pd(0) after the first Sonogashira coupling. The CA–RE reactivity of the 6,6-bis(DMA-acetylene)-substituted pentafulvene **1** with TCNE was investigated, and the transformation afforded an unanticipated dihydropentalene (±)-**3** as sole product in very high yield. The formation of this unexpected compound, which was also characterized by X-ray diffraction, presumably involves an initial CA–RE reaction, which is then followed by a formal 8-π electrocyclization reaction at room temperature. The opto-electronic properties of **1**-(±)-**3** were investigated by UV/Vis spectroscopy and electrochemistry. Sapphire-colored **2** features high-intensity absorptions spanning across the entire visible region and shows a low HOMO-LUMO gap of 1.41 eV (CV), whereas the gaps for (±)-**3** (1.64 eV) and **1** (2.08 eV) are larger. The low electrochemical gap of **2** originates from both a high HOMO and a low LUMO energy whereas compound (±)-**3** features the most anodically shifted first reduction potential (E_{red} = –1.08 V) and the lowest LUMO energy. The new chromophores are now being investigated for opto-electronic applications and the scope of the transformations, which lead to their formation, is explored in more detail.

4. Experimental section

4.1. General considerations

4.1.1. Physical characterization. ^{1}H and ^{13}C NMR spectra were taken on a Varian AV 400 or a Bruker DRX 600 spectrometer. Spectra were referenced to residual solvent peaks. Chemical shifts are expressed in parts per million (δ). Coupling constants (J) are expressed in Hertz. Coupling patterns are designated as s, singlet; d, doublet; t, triplet; m, multiplet. UV/Vis spectra were recorded on a Varian Cary-500 spectrophotometer; path lengths of 1 mm were used. Wavelengths are reported in nanometers and molar extinction coefficients ε in L mol^{-1} cm^{-1}. IR spectra were recorded on a Perkin Elmer BX FT-IR spectrophotometer; peaks are reported in wavenumbers (cm^{-1}). Mass spectrometry was performed by the MS-service at ETH Zürich. High resolution matrix-assisted laser-desorption-ionization (HR-MALDI) mass spectra were measured on a Varion Ionspec Ultima MALDI-FTICR mass spectrometer using trans-2-[3-(4-tertbutylphenyl)-2-methyl-2-propenylidene]malononitrile (DCTB) as matrix. Electrospray ionization mass spectrometry (ESI–MS) was performed on a Bruker Daltonics maXis (UHR–TOF).

4.1.2. Electrochemical measurements. All electrochemical measurements were performed with an Autolab PGSTAT 12 (Metrohm) and a conventional three-electrode system, comprising a glassy carbon (GC) substrate as working electrode, a platinum wire as the auxiliary electrode, and SCE electrode (Metrohm) as reference. The GC electrodes were purchased from CH Instrument, Inc. (Tx, USA) as 2-mm-diameter rods. The electrodes were polished successively with 1.0, 0.3, and 0.05 μm alumina slurry made from dry alumina powder and Milli-Q water on microcloth pads

(CH Instruments, Inc. Tx, USA). They were thoroughly rinsed with Milli-Q water, acetone and ethanol, and dried with an argon gas stream, before measurements.

4.1.3. Single-crystal X-ray crystallography. Detailed information on the X-ray crystal analysis is included in the Supporting Information. Crystallographic data have been deposited with the Cambridge Crystallographic Data Centre as supplementary publication nos. CCDC 1044103 (**1**), CCDC 1044102 (**2**), CCDC 1044105 ((±)-**3**) and CCDC 1044104 (**4**). Copies of the data can be obtained, free of charge, on application to CCDC, 12 Union Road, Cambridge CB2 1EZ, UK (fax: +44 (0)1223336033 or e-mail: deposit@ccdc.cam.ac.uk).

4.2. Compound 4

A two-neck flask under a nitrogen atmosphere was charged with tetraphenylcyclopentadienone (2.50 g, 6.50 mmol) and carbon tetrabromide (3.23 g, 9.75 mmol). Dry dichloromethane (56 ml) was added, and the solution was cooled to 0 ℃. Triisopropyl phosphite (4.8 mL, 19.5 mmol) was added dropwise, and the solution was stirred for 4.5 h at 0 ℃. Then the solution was warmed and stirred at rt for 24 h. The reaction was quenched with 120 mL of a saturated aqueous $NaHCO_3$ solution. The aqueous layer was extracted once with CH_2Cl_2, and the combined organic layers were washed with brine twice. The organic layer was dried over $MgSO_4$, and the solvent was evaporated. The residue was purified by column chromatography (SiO_2, pentane/dichloromethane from 10:0 to 3:7). Compound **4** was obtained as red powder in 18% yield (636 mg, 1.18 mmol). R_f = 0.74 (SiO_2, CH_2Cl_2/hexane 1:1); mp = 184-185 ℃; ^{1}H NMR (400 MHz, $CDCl_3$) δ = 7.29-7.20 (m,

10H), 7.03-6.95 (m, 6H), 6.84-6.82 (m, 4H); ^{13}C NMR (100 MHz, $CDCl_3$) δ = 146.4, 146.3, 136.7, 134.8, 134.6, 131.7, 130.0, 128.1, 127.2, 127.1, 126.8, 104.2; UV/Vis (CH_2Cl_2) λ_{max} (ε) 261 (1.9 x 10^4), 324 (1.5 x 10^4); IR (ATR): v = 3054 (w), 2920 (w), 2151 (w), 1608 (w), 1519 (w), 1485 (w), 1440 (w), 1345 (w),1239 (w), 1114 (w), 1073 (w), 1027 (w), 912 (w), 865 (w), 840 (w), 790 (w), 776 (w),754 (w), 737 (w), 725 (w), 693 (m); HR-MS (MALDI/ESI) Calculated for $C_{30}H_{21}{}^{79}Br_2$ $[M+H]^+$ 539.0005, found 539.0006.

4.3. Compounds 1 and 2

A two-neck flask was charged with compound **4** (540 mg, 1.00 mmol), 4-ethynyl-*N*,*N*-dimethylaniline (305 mg, 2.10 mmol), and triethylamine (34 mL). After the solution was degassed, $[PdCl_2(PPh_3)_2]$ (14 mg, 0.02 mmol) and CuI (9 mg, 0.045 mmol) were added and the solution was stirred under a nitrogen atmosphere for 21 h. The solvent was evaporated, and the residue was purified by column chromatography (SiO_2, pentane/CH_2Cl_2 from 10:0 to 6:4). Compound **1** was obtained as a red solid in 22% yield (150 mg, 0.22 mmol), and compound **2** was isolated as a deep blue thin powder in 18% yield (123 mg, 0.18 mmol). Data of compound **1**: R_f = 0.44 (SiO_2, CH_2Cl_2/hexane 1:1); mp = 248-249 ℃ (dec.); ^{1}H NMR (400 MHz, $CDCl_3$) δ = 7.41-7.38 (m, 4H), 7.25-7.17 (m, 6H), 7.00-6.94 (m, 6H), 6.79-6.75 (m, 8H), 6.47 (d, 4H, J = 8.1 Hz), 2.96 (s, 12H); ^{13}C NMR (100 MHz, $CDCl_3$) δ = 150.6, 147.0, 143.5, 137.5, 135.8, 134.0, 133.0, 132.0, 130.6, 127.6, 127.0, 126.4, 126.1, 115.3, 111.2, 109.3, 106.5, 90.7, 40.2; UV/Vis (CH_2Cl_2) λ_{max} (ε) 285 (4.0 x 10^4), 491 (5.1 x 10^4); IR (ATR): v = 3054 (w), 2893 (w), 2851 (w), 2179 (m), 2146 (s), 1882 (w), 1601 (s), 1542 (m), 1521 (s), 1505 (s), 1492 (s), 1480 (s), 1439 (s), 1357 (s), 1333 (m), 1290 (m), 1230 (s), 1188 (s), 1152 (s), 1116 (s), 1085 (s), 1070 (m), 1027 (m), 1004 (w), 942 (s), 853 (w), 808 (s), 791 (m), 772 (m), 762 (m), 752 (m), 733 (s), 703 (s),

691 (s), 658 (m), 644 (m), 632 (m), 619 (m), 611 (m); HR-MS (MALDI/ESI) Calculated for $C_{50}H_{40}N_2Na$ $[M+Na]^+$ 691.3084, found 691.3080; calculated for $C_{50}H_{40}KN_2$ $[M+K]^+$ 707.2823, found 707.2819.

Data of compound **2**: R_f = 0.38 (SiO_2, CH_2Cl_2/hexane 1:1); mp = 243-244 ℃ (dec.); ^1H NMR (400 MHz, $CDCl_3$) δ = 7.53 (d, 2H, J = 8.5 Hz), 7.42-7.37 (m, 6H), 7.32-7.23 (m, 6H), 7.13-7.11 (m, 6H), 7.01-6.97 (m, 4H), 6.69 (d, 2H, J = 8.5 Hz), 6.54 (d, 2H, J = 8.5 Hz), 3.07 (s, 6H), 3.06 (s, 6H); ^{13}C NMR (100 MHz, $CDCl_3$) δ = 151.7, 150.9, 148.8, 142.1, 140.9, 140.7, 136.5, 136.5, 136.3, 135.9, 134.0, 133.1, 132.9, 131.3, 130.8, 130.8, 130.8, 130.4, 127.8, 127.7, 127.6, 127.5, 126.3, 126.2, 126.1 125.8 125.7, 122.5, 116.9, 111.8, 111.5, 109.2, 103.9, 88.6, 40.3, 40.3; UV/Vis (CH_2Cl_2) λ_{max} (ε) 291 (4.4 x 10^4), 540 (3.9 x 10^4), 631 (4.4 x 10^4); IR (ATR): v = 3642 (w), 3057 (w), 2917 (m), 2849 (m), 2164 (s), 2039 (s), 1594 (s), 1519 (s), 1494 (s), 1468 (s), 1438 (s), 1367 (s), 1345 (s), 1313 (s), 1267 (s), 1225 (s), 1187 (s), 1153 (s), 1088 (s), 1067 (s), 1025 (s), 1001 (s), 962 (s), 946 (s), 911 (s), 847 (m), 810 (s), 790 (s), 775 (s), 760 (s), 740 (s), 716 (s), 691 (s), 664 (s), 627 (s), 615 (s); HR-MS (MALDI/ESI) Calculated for $C_{50}H_{40}N_2Na$ $[M+Na]^+$ 691.3084, found 691.3080.

4.4. Compound (±)-3

Compound **1** (30 mg, 0.04 mmol) was dissolved in CH_2Cl_2 (8 mL), and tetracyanoethylene (5 mg, 0.04 mmol) was added. After 5 h, the solvent was evaporated and the residue purified by column chromatography (SiO_2, pentane/CH_2Cl_2 from 1:0 to 0:1). Compound (±)-**3** was obtained as a dark purple solid in 81% yield (26 mg, 0.03 mmol). R_f = 0.59 (SiO_2, CH_2Cl_2); mp = 268-270 ℃ (dec.); ^1H NMR (400 MHz, $CDCl_3$) δ = 7.55 (d, 2H, J = 8.5 Hz), 7.43 (d, 2H, J = 6.5

Hz), 7.36-3.34 (m, 3H), 7.31-7.25 (m, 6H), 7.22-7.20 (m, 4H), 7.15 (d, 2H, *J* = 7.5 Hz), 7.11 (d, 1H, *J* = 7.5 Hz), 7.06 (t, 2H, *J* = 7.3 Hz), 6.90 (d, 2H, *J* = 7.5Hz), 6.76 (d, 2H, *J* = 7.8 Hz), 6.62 (d, 2H, *J* = 8.5 Hz), 3.10 (s, 6H), 3.04 (s, 6H); ^{13}C NMR (100 MHz, $CDCl_3$) δ = 161.8, 153.6, 151.7, 150.4, 148.8, 148.2, 135.6, 135.2, 134.3, 133.9, 133.5, 133.3, 132.2, 130.7, 130.5, 130.5, 129.8, 129.6, 129.0, 128.5, 128.5, 128.0, 127.8, 119.5, 115.6, 114.8, 114.6, 113.9, 112.3, 111.7, 111.6, 107.2, 84.6, 81.0, 79.1, 48.2, 40.2, 40.1; UV/Vis (CH_2Cl_2) λ_{max} (ε) 337 (2.4 x 10^4), 489 (1.8 x 10^4); IR (ATR) *v* = 2920 (w), 2855 (w), 2216 (w), 2162 (m), 1598 (s), 1531 (m), 1492 (m), 1479 (m), 1443 (m), 1368 (s), 1324 (w), 1283 (w), 1232 (w), 1201 (w), 1180 (s), 1165 (s), 1125 (s), 1065 (m), 1029 (w), 1000 (w), 945 (w), 871 (w), 827 (w), 827 (w), 812 (m), 780 (w), 765 (w), 755 (w), 737 (m), 730 (m), 697 (s), 671 (m); HR-MS (MALDI/ESI) Calculated for $C_{56}H_{41}N_6$ $[M+H]^+$ 797.3387, found 797.3395; calculated for $C_{56}H_{40}N_6Na$ $[M+Na]^+$ 819.3207, found 819.3210; calculated for $C_{56}H_{40}KN_6$ $[M+K]^+$ 835.2944, found 835.2944.

Acknowledgments

This work was supported by the Swiss National Science Foundation and the ERC Advanced Grant No. 246637 (“OPTELOMAC”). We thank the French Ministry of Higher Education and Research for awarding a Ph.D. fellowship to N.K.

Supplementary data

Detailed information of the X-ray crystal analysis, crystallographic data for **1**, **2** and (±)-**3**. Electrochemical analysis and cyclic voltammograms of **1**, **2** and (±)-**3**. Supplementary data associated with this article can be found in the online version, at **http://dx.doi.org/**

References and notes

1. (a) Wu, X.; Wu, J.; Liu, Y.; Jen, A. K. Y. *J. Am. Chem. Soc.* **1998**, *121*, 472-473; (b) Mochida, T.; Yamazaki, S. *J. Chem. Soc., Dalton Trans.* **2002**, 3559-3564; (c) Morioka, Y.; Yoshizawa, N.; Nishida, J.-i.; Yamashita, Y. *Chem. Lett.* **2004**, *33*, 1190-1191; (d) Michinobu, T.; May, J. C.; Lim, J. H.; Boudon, C.; Gisselbrecht, J.-P.; Seiler, P.; Gross, M.; Biaggio, I.; Diederich, F. *Chem. Commun.* **2005**, 737–739; (e) Shoji, T.; Ito, S.; Toyota, K.; Yasunami, M.; Morita, N. *Chem.–Eur. J.* **2008**, *14*, 8398 –8408 ; (f) Shoji, T.; Higashi, J.; Ito, S.; Okujima, T.; Yasunami, M.; Morita, N. *Chem.–Eur. J.* **2011**, *17*, 5116– 5129 (g) Koszelewski, D.; Nowak-Król, A.; Gryko, D. T. *Chem.–Asian J.* **2012**, *7*, 1887-1894; (h) García, R.; Herranz, M. Á.; Torres, M. R.; Bouit, P.-A.; Delgado, J. L.; Calbo, J.; Viruela, P. M.; Ortí, E.; Martín, N. *J. Org. Chem.* **2012**, *77*, 10707-10717; (i) Betou, M.; Kerisit, N.; Meledje, E.; Leroux, Y. R.; Katan, C.; Halet, J.-F.; Guillemin, J.-C.; Trolez, Y. *Chem.–Eur. J.* **2014**, *20*, 9553-9557.
2. (a) Jayamurugan, G.; Gisselbrecht, J.-P.; Boudon, C.; Schoenebeck, F.; Schweizer, W. B.; Bernet, B.; Diederich, F. *Chem. Commun.* **2011**, *47*, 4520-4522; (b) Reisinger, C. M.; Rivera-Fuentes, P.; Lampart, S.; Schweizer, W. B.; Diederich, F. *Chem.–Eur. J.* **2011**, *17*, 12906-12911; (c) Shoji, T.; Ito, S.; Okujima, T.; Morita, N. *Org. Biomol. Chem.* **2012**, *10*, 8308-8313; (d) Jayamurugan, G.; Finke, A. D.; Gisselbrecht, J.-P.; Boudon, C.; Schweizer, W. B.; Diederich, F. *J. Org. Chem.* **2014**, *79*, 426-431; (e) Gawel, P.; Dengiz, C.; Finke, A. D.; Trapp, N.; Boudon, C.; Gisselbrecht, J.-P.; Diederich, F. *Angew. Chem. Int. Ed.* **2014**, 53, 4341-4345.
3. (a) Andrew, T. L. ; Cox, J. R.; Swager, T. M. *Org. Lett.* **2010**, *12*, 5302-5305; (b) Andrew, T. L.; Bulovic, V. *ACS Nano* **2012**, *6*, 4671-4677.
4. Finke, A. D.; Haberland, S.; Schweizer, W. B.; Chen, P.; Diederich, F. *Angew. Chem. Int. Ed.* **2013**, *52*, 9827-9830; (b) Finke, A. D.; Diederich, F. *Chem. Record* **2015**, *15*, 19-30.
5. Finke, A. D.; Dumele, O.; Zalibera, M.; Confortin, D.; Cias, P.; Jayamurugan, G.; Gisselbrecht, J.-P.; Boudon, C.; Schweizer, W. B.; Gescheidt, G.; Diederich, F. *J. Am. Chem. Soc.* **2012**, *134*, 18139-18146.
6. Jayamurugan, G.; Dumele, O.; Gisselbrecht, J.-P.; Boudon, C.; Schweizer, W. B.; Bernet, B.; Diederich, F. *J. Am. Chem. Soc.* **2013**, *135*, 3599-3606.

7. (a) Möllerstedt, H.; Piqueras, M. C.; Crespo, R.; Ottosson, H. *J. Am. Chem. Soc.* **2004**, *126*, 13938–13939; b) Ottosson, H.; Kilså, K.; Chajara, K.; Piqueras, M. C.; Crespo, R.; Kato, H.; Muthas, D. *Chem.–Eur. J.* **2007**, *13*, 6998-7005; (c) Dahlstrand, C.; Yamazaki, K.; Kilså, K.; Ottosson, H. *J. Org. Chem.* **2010**, *75*, 8060–8068; (d) Endo, Y.; Hasegawa, M.; Matsui, T.; Yagi, H.; Hino, S.; Mazaki, Y. *Org. Lett.* **2014**, *16*, 5608–5611.

8. Gholami, M.; Ramsaywack, S.; Chaur, M. N.; Murray, A. H.; McDonald, R.; Ferguson, M. J.; Echegoyen, L.; Tykwinski, R. R. *Chem.–Eur. J.* **2013**, *19*, 15120-15132.

9. (a) Toda, T.; Shimazaki, N.; Mukai, T. *Angew. Chem. Int. Ed.* **1987**, *26*, 335-336; (b) Iyoda, M.; Tanake, S.; Nishioka, K.; Oda, M. *Tetrahedron Lett.* **1983**, *24*, 2861-2864.

10. (a) Dehu, C.; Meyers, F.; Brédas, J. L. *J. Am. Chem. Soc.* **1993**, *115*, 6198-6206; (b) Quinoid character δ*r* was calculated for DMA moieties with the following formula: δr = [(a+a'+c+c')/4] - [(b+b')/2]. For benzene, δr = 0; for fully quinoid rings, δr = 0.10−0.12 Å.

11. (a) Bouvy, D.; Janousek, Z.; Viehe, H. G. *Tetrahedron Lett.* **1993**, *34*, 1779-1782; (b) Tinant, B.; Declercq, J.-P.; Bouvy, D.; Janousek, Z.; Viehe, H. G. *J. Chem. Soc., Perkin Trans. 2* **1993**, 911-915; (c) Wu, Y.-L.; Tancini, F.; Schweizer, W. B.; Paunescu, D.; Boudon, C.; Gisselbrecht, J.-P.; Jarowski, P. D.; Dalcanale, E.; Diederich, F. *Chem. Asian J.* **2012**, *7*, 1185-1190.

12. (a) Berkovitch-Yellin, Z.; Leiserowitz, L. *Acta Crystallogr., Sect. B: Struct. Sci.* **1977**, *33*, 3657-3669; (b) Januszewski, J. A.; Wendinger, D.; Methfessel, C. D.; Hampel, F.; Tykwinski, R. R. *Angew. Chem. Int. Ed.* **2013**, *52*, 1817-1821; (c) Ueta, S.; Hida, K.; Nishiuchi, M.; Kawamura, Y. *Org. Biomol. Chem.* **2014**, *12*, 2784-2791.

13. (a) Elsevier, C. J.; Kleijn, H.; Ruitenberg, K.; Vermeer, P. *J. Chem. Soc., Chem. Commun.* **1983**, 1529-1530; (b) Elsevier, C. J.; Kleijn, H.; Boersma, J.; Vermeer, P. *Organometallics* **1986**, *5*, 716-720; (c) Tsuji, J.; Mandai, T. *Angew. Chem. Int. Ed.* **1995**, *34*, 2589-2612.

14. (a) Kaiser, R.; Hafner, K. *Angew. Chem. Int. Ed.* **1970**, *9*, 892-893; (b) Gajewski, J. J.; Cavender, C. J. *Tetrahedron Lett.* **1971**, *16*, 1057-1060.

15. Jarowski, P. D.; Wu, Y.-L.; Boudon, C.; Gisselbrecht, J.-P.; Gross, M.; Schweizer, W. B.; Diederich, F. *Org. Biomol. Chem.* **2009**, *7*, 1312-1322.

Table of contents

A 6,6-bis[(4-*N,N*-dimethylanilino)ethynyl]pentafulvene has been prepared using a 6,6-dibromopentafulvene and 4-ethynyl-*N,N*-dimethylaniline under Sonogashira cross-coupling conditions. A push-pull [3]cumulene was formed unexpectedly during this reaction in moderate yield. The 6,6-bis[(4-*N,N*-dimethylanilino)ethynyl]pentafulvene was reacted with tetracyanoethylene, and an unprecedented 1,2-dihydropentalene was obtained in high yield as the exclusive product.

Graphical Abstract

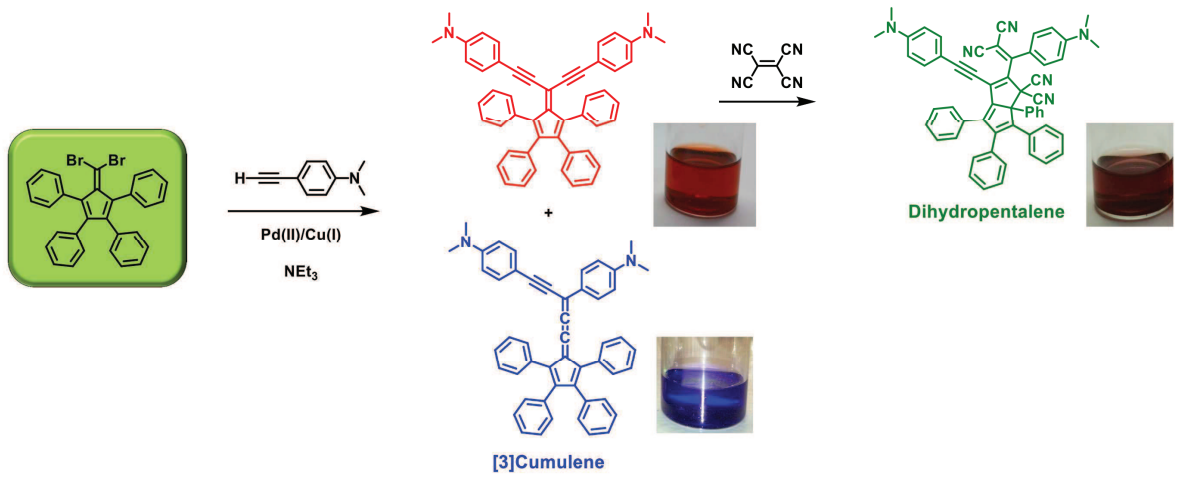

ACCEPTED MANUSCRIPT

Tetrahedron

journal homepage: www.elsevier.com

Supporting Information

New reactivity of 6,6-bis-donor-substituted pentafulvenes: one-step synthesis of highly substituted [3]cumulene and dihydropentalene

Nicolas Kerisit,[1] Aaron D. Finke,[2] Nils Trapp,[2] Yann R. Leroux,[3] Jean-Claude Guillemin,[1] Yann Trolez,[1] François Diederich[2,*]

[1] Ecole Nationale Supérieure de Chimie de Rennes, CNRS, UMR 6226, 11 allée de Beaulieu, CS 50837, 35708 Rennes Cedex 7, France

[2] Laboratorium für Organische Chemie, ETH Zurich, Vladimir-Prelog-Weg 3, 8093 Zurich, Switzerland. Email: diederich@org.chem.ethz.ch

[3] Institut des Sciences Chimiques de Rennes, CNRS, Université de Rennes 1, UMR 6226, Campus de Beaulieu, 35042 Rennes Cedex, France

Table of Contents

1. Electrochemistry

All electrochemical measurements were performed with an Autolab PGSTAT 12 (Metrohm) and a conventional three-electrode system, comprising a glassy carbon (GC) substrate as working electrode, a platinum wire as the auxiliary electrode, and SCE electrode (Metrohm) as reference. The GC electrodes were purchased from CH Instrument, Inc. (Tx, USA) as 2-mm-diameter rods. The electrodes were polished successively with 1.0, 0.3, and 0.05 μm alumina slurry made from dry alumina powder and Milli-Q water on microcloth pads (CH Instruments, Inc. Tx, USA). They were thoroughly rinsed with Milli-Q water, acetone, and ethanol. The electrodes were dried with an argon gas stream, before measurements.

1.1. Cathodic cyclic voltammograms

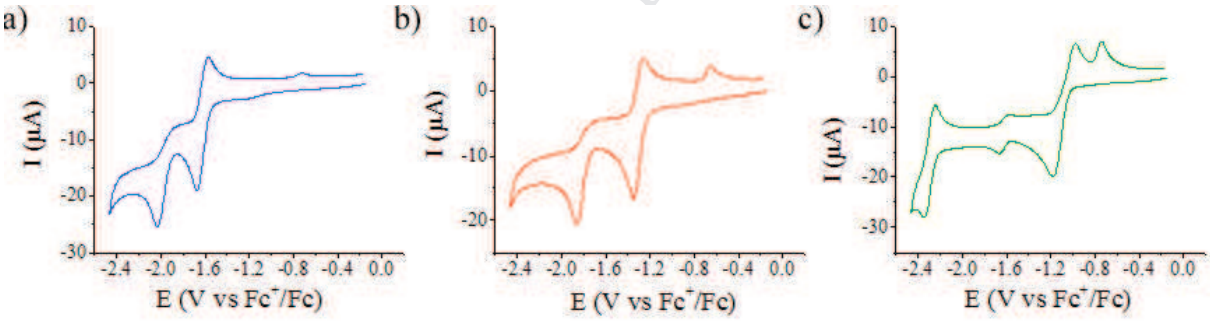

Figure 1SI. Cathodic cyclic voltammograms obtained at a scan rate of 0.1 V s^{-1} in CH_2Cl_2 + 0.2 M Bu_4NPF_6 on a glassy carbon working electrode of compounds **1** (a, blue line), **2** (b, red line), and (±)-**3** (c, green line). Scan rate = 100 mV s^{-1}. All potentials are given versus the Fc^+/Fc couple used as external standard.

1.2. Anodic cyclic voltammograms

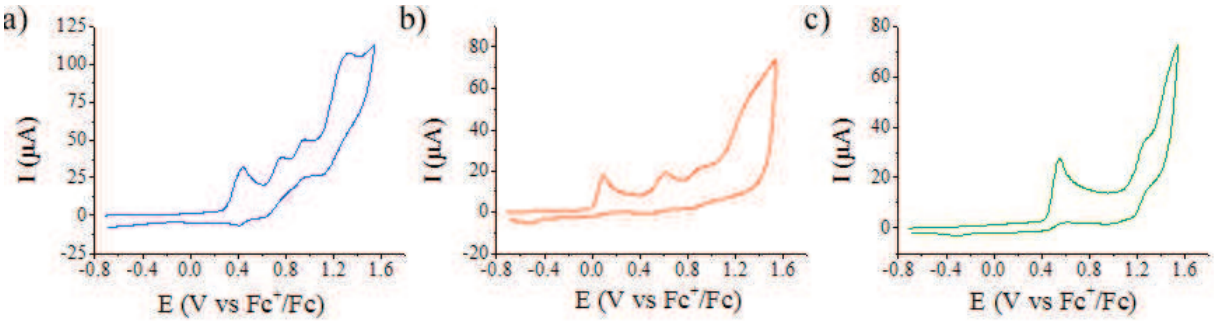

Figure 2SI. Anodic cyclic voltammograms obtained at a scan rate of 0.1 V s^{-1} in CH_2Cl_2 + 0.2 M Bu_4NPF_6 on a glassy carbon working electrode of compounds **1** (a, blue line), **2** (b, red line), and (±)-**3** (c, green line). Scan rate = 100 mV s^{-1}. All potentials are given versus the Fc^+/Fc couple used as external standard.

1.3. Electrochemical analysis

As recently pointed out in the literature,[1] many different methods can be used to determine HOMO and LUMO energy levels from electrochemical measurements. For clarity and comparison with other molecules in the literature, we will describe here the methodology and calculations performed to access these energy levels.

Initially, Bredas *et al.*[2] proposed some empirical relations between ionization potential (IP), electron affinity (EA), and the onset redox potential measured by electrochemistry. These relations were obtained by fitting Valence Effective Hamiltonian (VEH) calculations to the corresponding experimental data. These empirical relations are often used without correction.

$$IP = E_{Onset}^{Ox} + 4.4(eV) \qquad (1)$$

$$EA = E_{Onset}^{Red} + 4.4(eV) \qquad (2)$$

Here, onset potentials will be not taken into account, as it is more appropriate for the study of polymers, or more generally molecules deposited onto surfaces. We prefer to use here half-wave potential $E_{1/2}$ (which is a good estimation of the formal potential, $E^{0'}$) as we are interested on freely diffusing molecules in solution. Trying to rationalize these equations, to estimate the IP and EA from the measured redox potentials, it is necessary to correlate the electrochemical potentials to the vacuum level. It is convenient to use the standard hydrogen electrode (SHE) as reference for the potential values (E), and then correct these potentials using the vacuum level reference. The conversion from SHE to the vacuum reference has been discussed originally by Trasatti,[3] who has determined the energy corresponding to the standard hydrogen electrode (SHE) as 4.6 ± 0.1 eV on the zero vacuum-level scale.[4]

$$E_{SHE/vacuum} = -4.6 \pm 0.1(eV) \qquad (3)$$

It is thus possible to calculate the IP and EA from the redox onset potential, relative to the vacuum level:

$$E_{Ag/AgCl} = E_{SHE} - 0.197(eV) \qquad (4)$$

$$E_{Ag/AgCl} = E_{VAC} + 4.403(eV) \qquad (5)$$

Assuming E_{vac} = 0, then EA = $e\,E_{1/2}^{Red}$, where e is the electron charge, this allows one to determine the IP and EA energies from the electrochemical experiments. One can notice that the empirical relations determined by Bredas *et al.* are valid for potentials measured versus Ag/AgCl reference electrode. We need here to add a correction since the potentials are measured versus SCE reference electrode and then expressed versus Fc^+/Fc redox couple as an external reference.[5]

$$E_{SCE} = E_{SHE} - 0.241(eV) \qquad (6)$$

$$E_{SCE} = E_{VAC} + 4.359(eV) \qquad (7)$$

$$E_{Fc^+/Fc} = E_{SCE} + 0.460(eV) \qquad (8)$$

From relation (1), (2) and (8) we obtain in our case:

$$IP = E_{1/2}^{Ox} + 4.819(eV) = -HOMO \qquad (9)$$

$$EA = E_{1/2}^{Red} + 4.819(eV) = -LUMO \qquad (10)$$

Table 1SI. Ionization potentials and electron affinities values for pentafulvalene **1**, [3]cumulene **2**, and dihydropentalene (±)-**3**.

Compound	*IP* (eV)	*EA* (eV)
1	5.23	3.19
2	4.92	3.51
(±)-**3**	5.38	3.74

The electrochemical energy gap, $\Delta E_{redox,}$ is calculated as the potential difference between the half-wave potential $E_{1/2}$ of the first oxidation and of the first reduction of the studied compound. As oxidation processes are not reversible for these compounds, peak potentials were chosen instead of $E_{1/2}$ for the calculation of ΔE_{redox}, which can introduce an error of approximately ±0.05 eV.

The optical energy gap, ΔE_{opt}, is defined as the energy corresponding to the onset wavelength (λ_{onset}) of the lowest-energy absorption. For clarity and comparison, we chose to take as λ_{onset}, the wavelength corresponding to 2.5% of the intensity of the maximum wavelength (λ_{max}) of the lowest energy absorption.

Table 2SI. λ_{onset} value and corresponding optical energy gap, ΔE_{opt}, for pentafulvalene **1**, [3]cumulene **2**, and dihydropentalene (±)-**3**.

Compound	λ_{onset} (nm)	ΔE_{opt} (eV)
1	620	2.00
2	850	1.46
(±)-**3**	728	1.70

2. X-Ray data

2.1. Instrumentation and refinement

Crystals of compounds were measured on a Bruker/Nonius APEX-II or a Bruker Kappa APEX-II Duo CCD diffractometer equipped with sealed tube Mo-K_α radiation (λ = 0.71073 Å, graphite monochromator) at 100 K. The structures were solved by direct methods with SHELXS and refined by full-matrix least-squares analysis using SHELXL with the program package Olex2.[14-16] Hydrogen atoms were restrained to idealized positions in terms of a riding model.

2.2. X-Ray crystal structure of compound 4 (CCDC 1044104)

Crystallogenesis: vapor diffusion of *n*-pentane into a CH_2Cl_2 solution at 4 °C, $C_{30}H_{20}Br_2$, M = 540.28 g mol^{-1}, monoclinic, Space group: *Pc*, a = 6.4541(3) Å, b = 11.8259(6) Å, c = 14.8702(8) Å, β = 91.197(2)°, V = 1134.73(10) Å^3, Z = 2, D_c = 1.581 g cm^{-3}, μ(Mo-K) = 3.588 mm^{-1}, F(000) = 540, T = 100 K, Reflections collected: 18632, Independent reflections: 4688 (R_{int} = 0.0278), Data/restraints/parameters:

4688/2/289, Final *R* indices (*I*>2 σ) R_1 = 0.0247, *R* indices (all data): wR_2 = 0.0593, Goodness-of-fit on F^2 of 0.974.

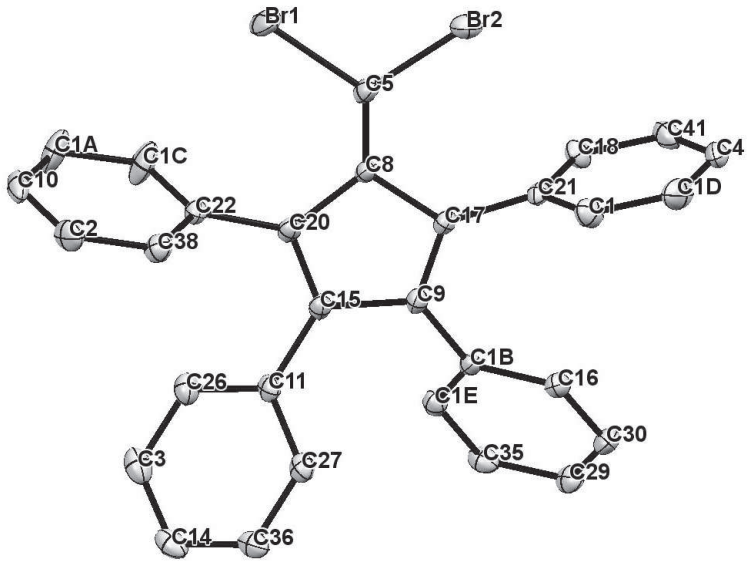

Figure 3SI. Crystal structure of compound **4**. Thermal ellipsoids of non-H atoms at 50% probability. Selected bond lengths (Å) and torsion angles (°): C5-C8 1.340(4), C8-C20 1.482(3), C8-C17 1.485(3), C9-C17 1.358(4), C9-C1B 1.480(3), C9-C15 1.486(3), C11-C27 1.396(4), C11-C26 1.397(4), C11-C15 1.477(4), C14-C3 1.382(4), C14-C36 1.385(4), C15-C20 1.355(3), C17-C21 1.487(3), C18-C21 1.381(4), C18-C41 1.383(4), C20-C22 1.487(3), C21-C1 1.379(4), C22-C38 1.388(4), C22-C1C 1.393(4), C26-C3 1.385(4), C27-C36 1.380(4), C29-C30 1.379(4), C29-C35 1.384(4), C30-C16 1.386(4), C35-C1E 1.381(4), C38-C2 1.393(4), C41-C4 1.368(4), C1-C1D 1.379(4), C2-C10 1.366(4), C4-C1D 1.381(5), C10-C1A 1.369(5), C16-C1B 1.409(3), C1A-C1C 1.384(4), C1B-C1E 1.391(4), C8-C20-C22-C1C 84.1(4), C27-C11-C15-C9 41.7(4), C17-C9-C1B-C16 41.7(4), C8-C17-C21-C1 92.8(3), Br2-C5-C8-C17 -6.6(4).

2.3. X-Ray crystal structure of compound 1 (CCDC 1044103)

Crystallogenesis: vapor diffusion of *n*-pentane into a CH_2Cl_2 solution at 4 °C, $C_{50}H_{40}N_2$, M = 668.84 g mol^{-1}, T = 100 K, monoclinic, Space group: $P2_1$, a = 6.3795(8) Å, b = 14.9657(19) Å, c = 18.793(3) Å, β = 93.088(3)°, V = 1791.6(4) Å^3, Z = 2, D_c = 1.240 g cm^{-3}, μ(Mo-K) = 0.071 mm^{-1}, F(000) = 708.0, Reflections collected: 16308, Independent reflections: 4269 (R_{int} = 0.0582), Data/restraints/parameters: 4269/1/473, Final R indices (I>2σ), R_1 = 0.0405, Final R indices (all data): wR_2 = 0.0813, Goodness-of-fit on F^2 of 1.011.

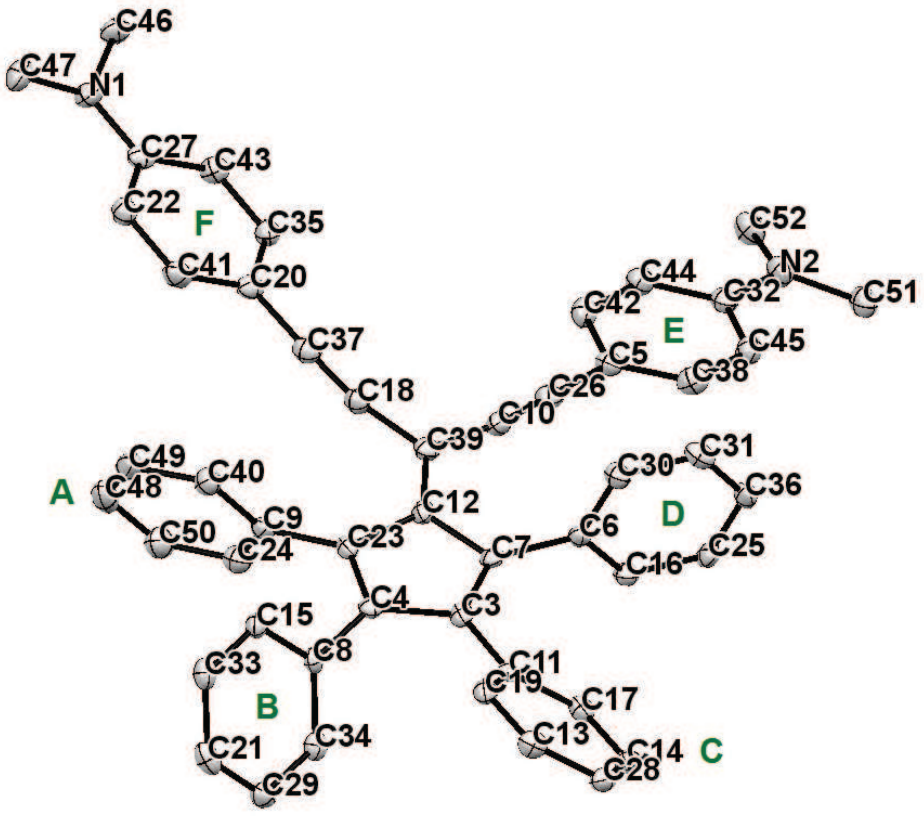

Figure 4SI. Crystal structure of compound **1**. Thermal ellipsoids of non-H atoms at 50% probability. Selected bond lengths (Å), torsion angles (°) and quinoid character δr (Å): C13-C19 1.394(3), C13-C28 1.377(3), C14-C17 1.381(3), C14-C28 1.380(3), C15-C33 1.388(3), C16-C25 1.382(3), C3-C4 1.482(3), C18-C37 1.207(3), C3-C7 1.376(3), C18-C39 1.424(3), C3-C11 1.479(3), C20-C35 1.404(3), C4-C8 1.479(3),

C20-C37 1.421(4), C4-C23 1.369(3), C20-C41 1.399(4), C5-C26 1.430(3), C21-C29 1.392(4), C5-C38 1.396(4), C21-C33 1.380(4), C5-C42 1.401(4), C22-C27 1.411(3), C6-C7 1.490(3), C22-C41 1.379(4), C6-C16 1.394(3), C24-C50 1.380(4), C6-C30 1.394(3), C25-C36 1.385(3), C7-C12 1.462(3), C27-C43 1.405(3), C8-C15 1.399(3), C29-C34 1.386(3), C8-C34 1.398(3), C30-C31 1.387(3), C9-C23 1.488(3), C31-C36 1.383(3), C9-C24 1.400(3), C32-C44 1.406(4), C9-C40 1.388(3), C32-C45 1.411(4), C10-C26 1.201(3), C35-C43 1.374(3), C10-C39 1.430(3), C38-C45 1.378(3), C11-C17 1.405(3), C40-C49 1.390(4), C11-C19 1.398(3), C42-C44 1.384(3), C12-C23 1.473(3), C48-C49 1.385(4), C12-C39 1.381(3), C48-C50 1.380(4), C12-C23-C9-C24 69.5(9), C3-C4-C8-C34 -54.0(5), C3-C4-C11-C19 -35.5(6), C12-C7-C6-C30 83.6(8), C12-C39-C20-C41 13.0(7), C12-C39-C5-C38 -14.7(5), δr (phenyl ring F) 0.028, δr (phenyl ring E) 0.022.

2.4. X-Ray crystal structure of compound 2•CH_2Cl_2 (CCDC 1044102)

Crystallogenesis: vapor diffusion of *n*-pentane into a CH_2Cl_2 solution at 4 °C, $C_{51}H_{42}Cl_2N_2$, M = 753.76 g mol^{-1}, T = 100 K, triclinic, Space group: P-1, a = 10.5547(15) Å, b = 11.9452(16) Å, c = 17.833(2) Å, α = 75.091(4)°, β = 76.590(5)°, γ = 65.991(4)°, V = 1964.0(5) Å^3, Z = 2, D_c = 1.275 g cm^{-3}, μ(Mo-K) = 0.204 mm^{-1}, F(000) = 792, Reflections collected: 33899, Independent reflections: 9130 (R_{int} = 0.0279), Data/restraints/parameters: 9130/30/519, Final R indices (I>2σ): R_1 = 0.0432, R indices (all data): wR_2 = 0.1514, Goodness-of-fit on F^2 of 1.104.

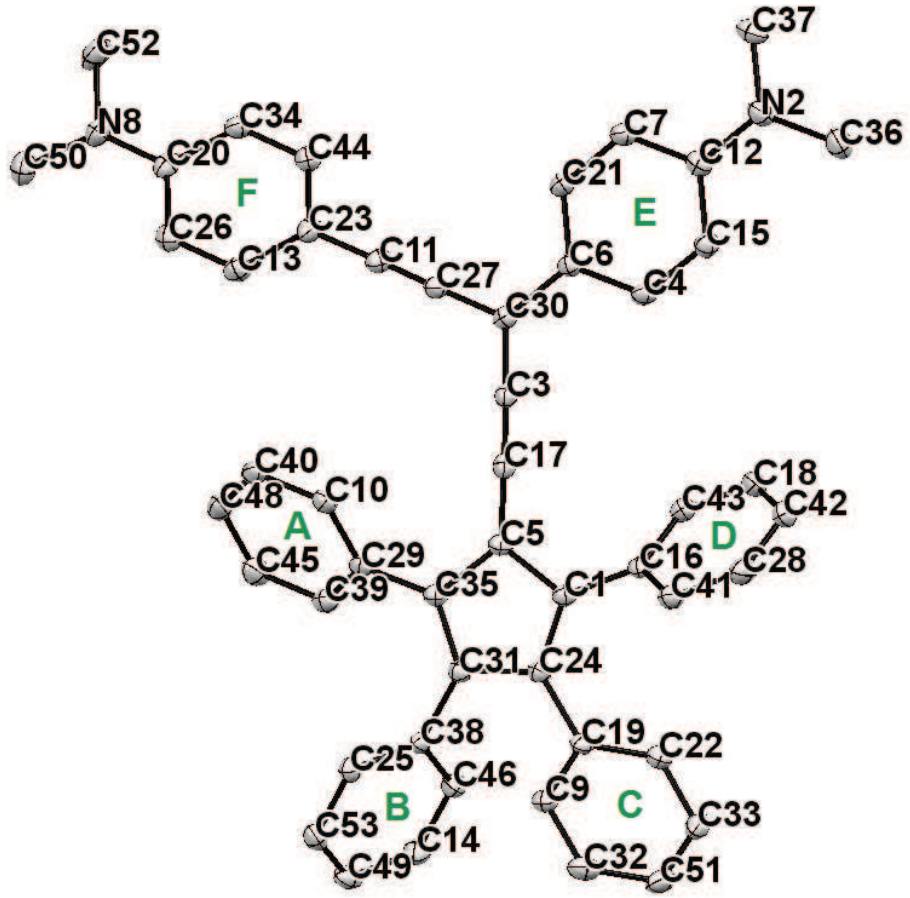

Figure 5SI. Crystal structure of compound **2** (solvent molecules are omitted for clarity). Thermal ellipsoids of non-H atoms at 50% probability. Selected bond lengths (Å), torsion angles (°) and quinoid character δr (Å): C1-C5 1.4589(18), C1-C16 1.4702(19), C1-C24 1.371(2), **C3-C17 1.230(2)**, **C3-C30 1.3641(19)**, C4-C6 1.4112(18), C4-C15 1.370(2), **C5-C17 1.3570(19)**, C5-C35 1.4578(19), C6-C21 1.395(2), C6-C30 1.444(2), C7-C12 1.4171(19), C7-C21 1.369(2), C9-C19 1.394(2), C9-C32 1.3863(19), C10-C29 1.401(2), C10-C40 1.3826(19), C11-C23 1.4237(18), C11-C27 1.2020(19), C12-C15 1.407(2), C13-C23 1.398(2), C13-C26 1.3729(19), C14-C46 1.383(2), C14-C49 1.377(2), C16-C41 1.395(2), C16-C43 1.397(2), C18-C42 1.380(2), C18-C43 1.383(2), C19-C22 1.398(2), C19-C24 1.4773(18), C20-C26 1.403(2), C20-C34 1.406(2), C22-C33 1.392(2), C23-C44 1.397(2), C24-C31 1.4668(18), C25-C38 1.389(2), C25-C53 1.387(2), C27-C30 1.4240(18), C28-C41

1.383(2), C28-C42 1.385(2), C29-C35 1.4691(18), C29-C39 1.398(2), C31-C35 1.3725(19), C31-C38 1.473(2), C32-C51 1.390(2), C33-C51 1.377(2), C34-C44 1.3775(19), C38-C46 1.395(2), C39-C45 1.3916(19), C40-C48 1.387(2), C45-C48 1.389(2), C49-C53 1.378(2), C10-C29-C35-C5 -43.8(2), C24-C31-C38-C46 -62.03(19), C22-C19-C24-C1 -49.6(2), C5-C1-C16-C43 -48.0(2), C4-C6-C30-C3 10.3(2), C13-C23-C30-C3 22.5(2), C27-C30-C5-C35 4.0(0), δr (phenyl ring F) 0.025, δr (phenyl ring E) 0.038.

2.5. X-Ray crystal structure of compound (±)-3•CH_2Cl_2 (CCDC 1044105)

Crystallogenesis: vapor diffusion of *n*-pentane into a CH_2Cl_2 solution at 4 °C, $C_{57}N_6Cl_2H_{42}$, M = 881.86 g mol^{-1}, T = 100 K, monoclinic, Space group: $C2/c$, a = 24.8188(15) Å, b = 10.1321(6) Å, c = 40.666(2) Å, β = 105.334(2) °, V = 9862.1(10) Å^3, Z = 8, D_c = 1.188 g cm^{-3}, μ(Mo-K) = 0.175 mm^{-1}, F(000) = 3680.0, Reflections collected: 8422, Independent reflections: 8422 (R_{int} = 0.0000), Data/restraints/parameters: 8422/8/597, Final R indices (I≥2σ): R_1 = 0.0600, Final R indices (all data): wR_2 = 0.1536, Goodness-of-fit on F^2 of 1.035.

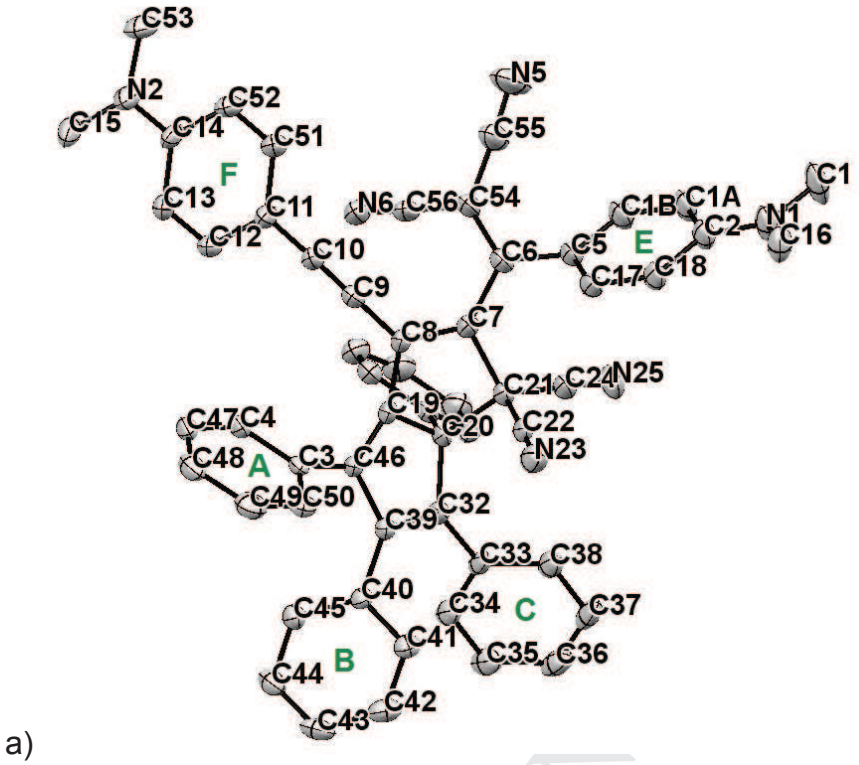

a)

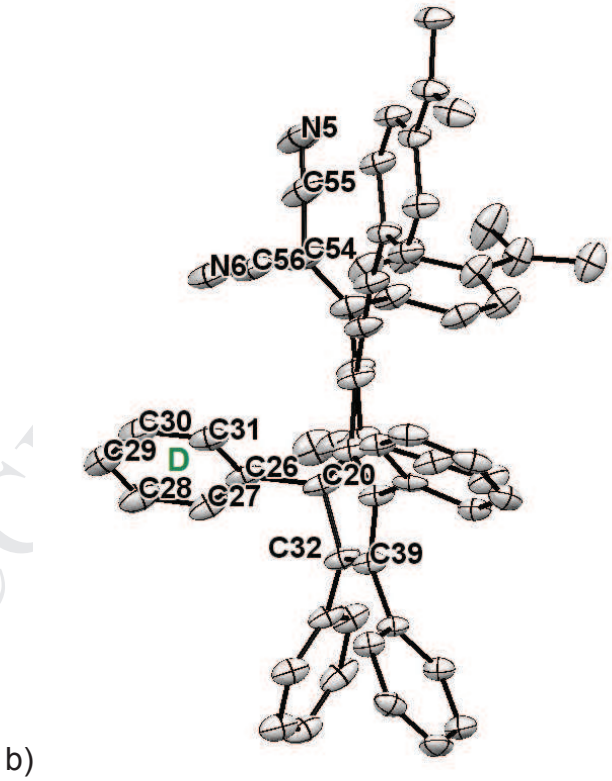

b)

Figure 6SI. Crystal structure of compound (±)-**3** (solvent molecules are omitted for clarity). Thermal ellipsoids of non-H atoms at 50% probability. Representation b) allows a better visualization of the phenyl ring pointing toward the back of the

molecule in representation a). Selected bond lengths (Å), torsion angles (°) and quinoid character δr (Å): C20-C32 1.516(3), C21-C22 1.494(3), C21-C24 1.476(3), C26-C27 1.393(3), C3-C4 1.393(3), C26-C31 1.400(3), C3-C46 1.468(3), C27-C28 1.376(4), C3-C50 1.392(3), C28-C29 1.387(3), C4-C47 1.388(3), C29-C30 1.370(4), C30-C31 1.390(4), C32-C33 1.484(3), C2-C1A 1.406(3), C32-C39 1.357(3), C2-C18 1.414(3), C33-C34 1.388(4), C1A-C1B 1.375(3), C33-C38 1.393(3), C1B-C5 1.400(3), C34-C35 1.382(3), C5-C6 1.469(3), C35-C36 1.384(3), C5-C17 1.397(3), C36-C37 1.372(4), C6-C7 1.444(3), C37-C38 1.387(3), C6-C54 1.379(3), C39-C40 1.482(3), C7-C8 1.379(3), C39-C46 1.481(3), C7-C21 1.543(3), C40-C41 1.392(3), C8-C9 1.413(3), C40-C45 1.393(3), C8-C19 1.446(3), C41-C42 1.380(3), C9-C10 1.208(3), C42-C43 1.377(3), C10-C11 1.417(3), C43-C44 1.379(3), C11-C12 1.390(3), C44-C45 1.382(3), C11-C51 1.406(3), C47-C48 1.372(4), C12-C13 1.378(3), C48-C49 1.385(3), C13-C14 1.411(3), C49-C50 1.387(3), C14-C52 1.406(4), C51-C52 1.372(3), C17-C18 1.374(3), C54-C55 1.430(4), C19-C20 1.512(3), C54-C56 1.435(4), C19-C46 1.354(3), C20-C21 1.598(3), C20-C26 1.532(3), C4-C3-C46-C19 55.4(3), C32-C39-C40-C41 54.0(3), C20-C32-C33-C38 61.4(3), C32-C20-C26-C27 63.3(3), C17-C5-C6-C7 42.3(3), C54-C6-C7-C8 42.2(3), C5-C6-C54-C55 12.1(4), C12-C11-C8-C19 15.3(2), δr (phenyl ring F) 0.028, δr (phenyl ring E) 0.030.

3. ^{1}H NMR and 13C NMR spectra of compounds 1-3

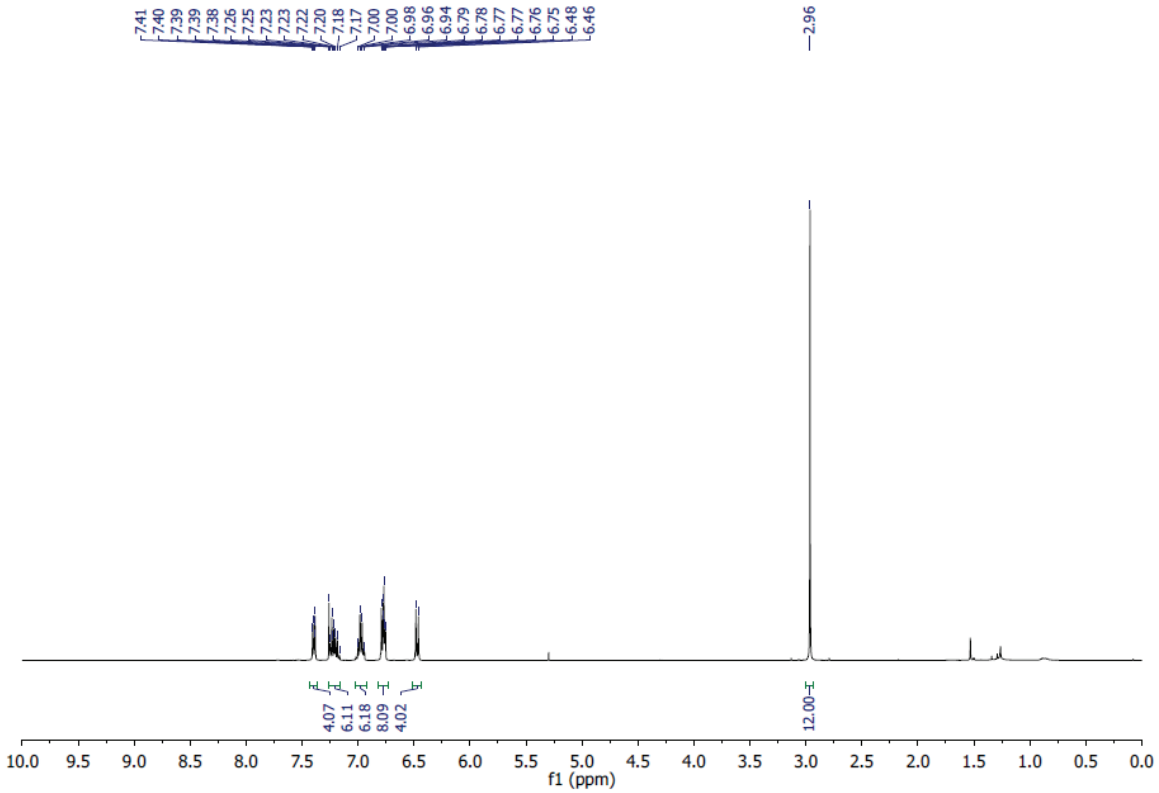

Figure 7SI. ^{1}H NMR ($CDCl_3$, 400 MHz) of **1**.

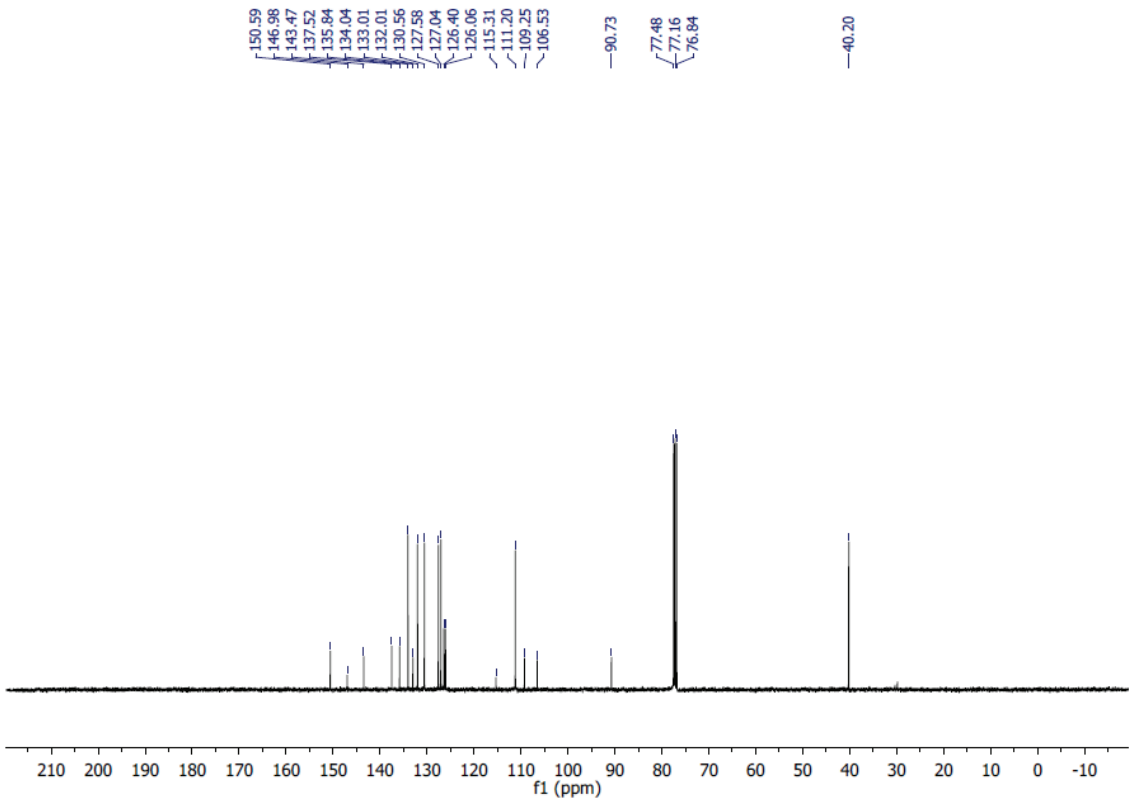

Figure 8SI. ^{13}C NMR ($CDCl_3$, 100 MHz) of **1**.

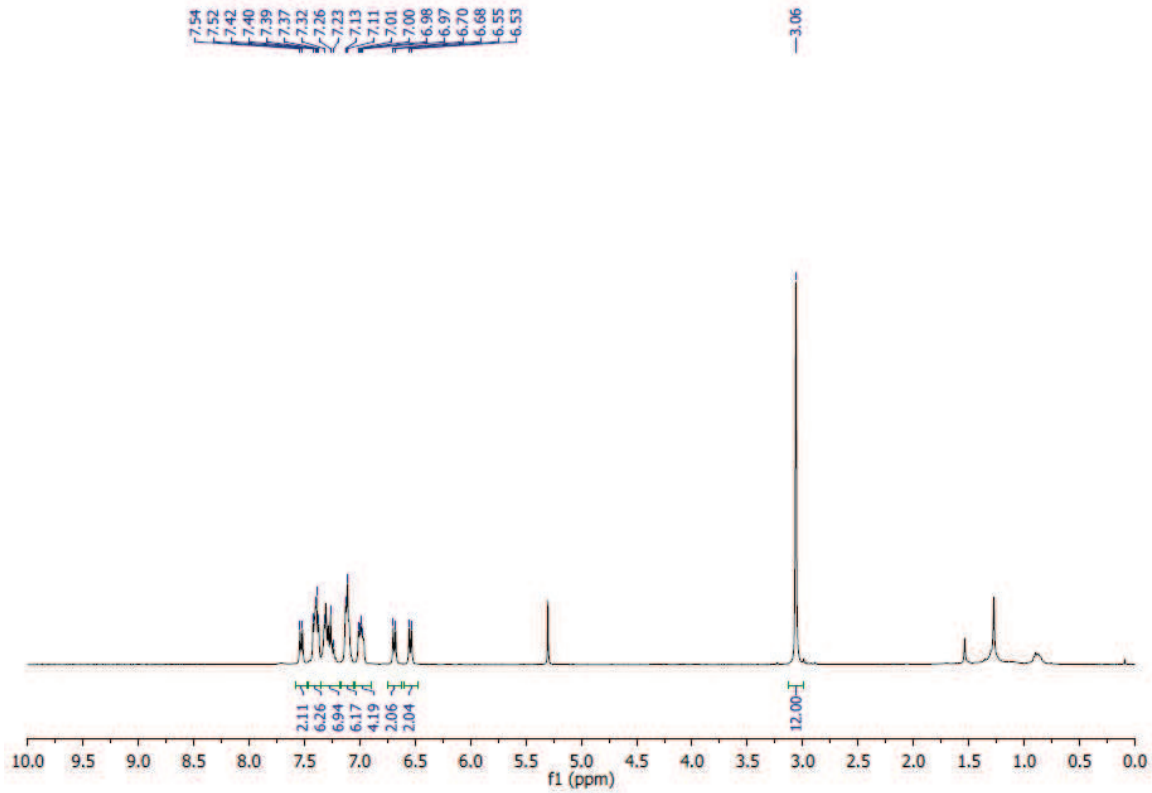

Figure 9SI. ^{1}H NMR ($CDCl_3$, 400 MHz) of **2**.

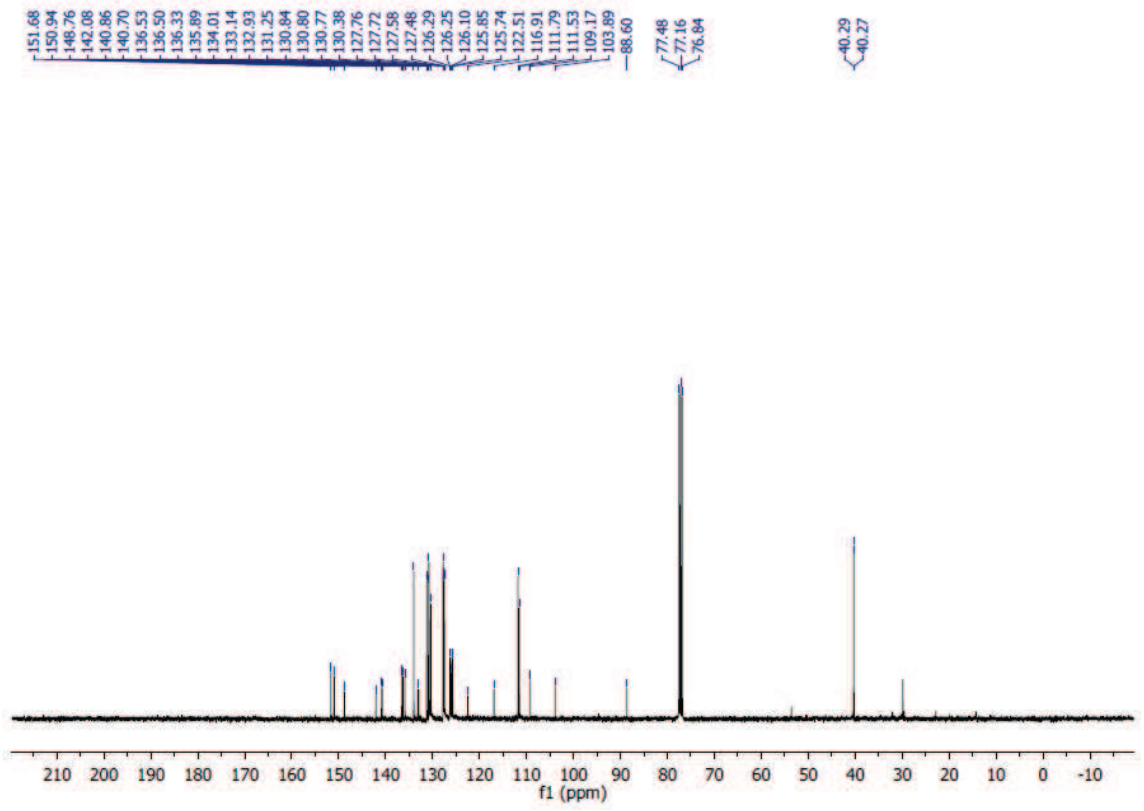

Figure 10SI. ^{13}C NMR ($CDCl_3$, 100 MHz) of **2**.

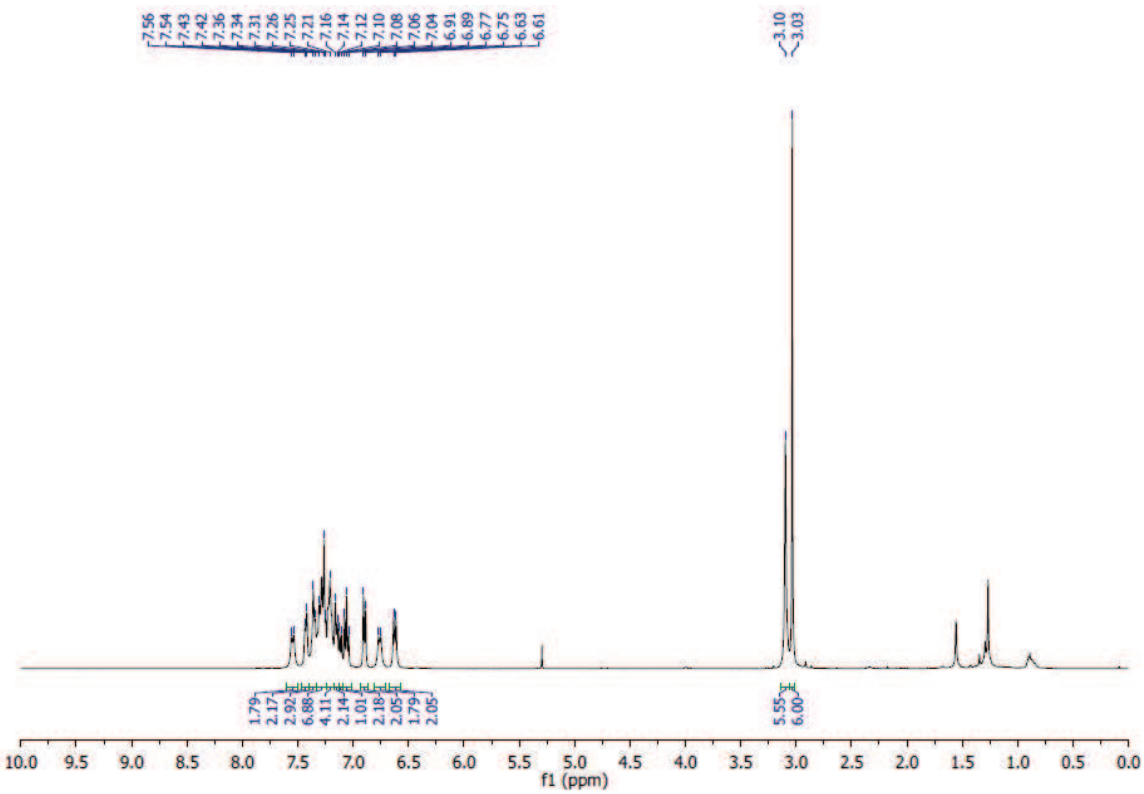

Figure 11SI. ^{1}H NMR ($CDCl_3$, 400 MHz) of (±)-**3**.

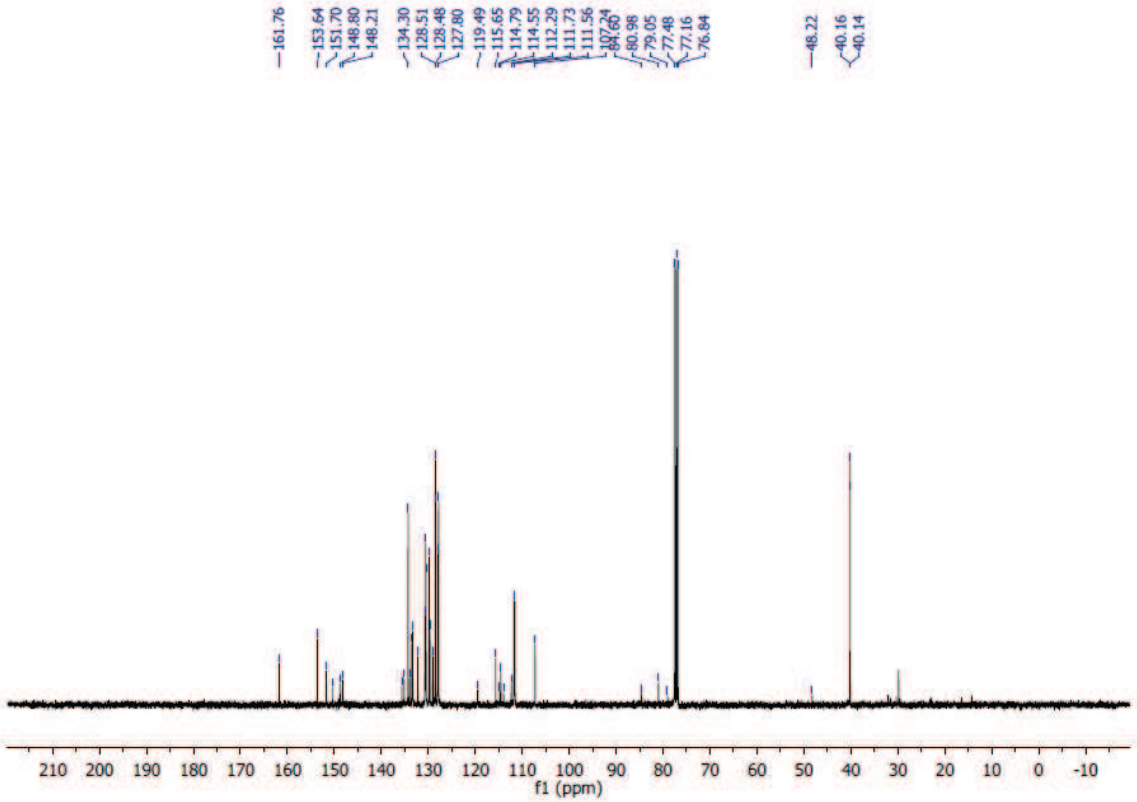

Figure 12SI. ^{13}C NMR ($CDCl_3$, 100 MHz) of (±)-**3**.

4. References

1. Cardona, C. M.; Li, W.; Kaifer, A. E.; Stockdale, D.; Bazan, G. C. Adv. Mater. **2011**, 23, 2367-2371.

2. Bredas, J. L.; Silbey, R.; Boudreaux, D. S.; Chance, R. R. *J. Am. Chem. Soc.* **1983**, *105*, 6555-6559.

3. Trasatti, S. *J. Electroanal. Chem. Interfacial Electrochem.* **1983**, *150*, 1-15.

4. Xie, Q.; Kuwabata, S.; Yoneyama, H. *J. Electroanal. Chem.* **1997**, *420*, 219-225.

5. Connelly, N. G.; Geiger, W. E. Chem. Rev. **1996**, 96, 877-910.

6. Dolomanov, O. V.; Bourhis, L. J.; Gildea, R. J.; Howard, J. A. K.; Puschmann, H. *J. Appl. Cryst.* **2009**, *42*, 339–341.

7. Sheldrick, G. M. *Acta. Cryst.* **2008**, *A64*, 112–122.

8. Sheldrick, G. M. *SHELXL-97, Program for the Refinement of Crystal Structures*. University of Göttingen, Germany, **1997**.